

Published in final edited form as:

Nitric Oxide. 2012 October 15; 27(3): 150–160. doi:10.1016/j.niox.2012.06.003.

A nanoparticle delivery vehicle for S-nitroso-N-acetyl cysteine: Sustained vascular response

Parimala Nacharaju^{a,1,*}, Chaim Tuckman-Vernon^{a,1}, Keith E. Maier^a, Jason Chouake^b, Adam Friedman^{a,b}, Pedro Cabrales^c, and Joel M. Friedman^a

^aPhysiology and Biophysics, Albert Einstein College of Medicine, Bronx, NY

^bDepartment of Medicine (Division of Dermatology), Montefiore Medical Center, Bronx, NY

^cDepartment of Bioengineering, University of California, San Diego, CA

Abstract

Interest in the development of nitric oxide (NO) based therapeutics has grown exponentially owing to its well elucidated and established biological functions. In line with this surge, S-nitroso thiol (RSNO) therapeutics are also receiving more attention in recent years both as potential stable sources of NO as well as for their ability to serve as S-nitrosating agents; S-nitrosation of protein thiols is implicated in many physiological processes. We describe two hydrogel based RSNO containing nanoparticle platforms. In one platform the SNO groups are covalently attached to the particles (SNO-np) and the other contains S-nitroso-N-acetyl cysteine encapsulated within the particles (NAC-SNO-np). Both platforms function as vehicles for sustained activity as trans-S-nitrosating agents. NAC-SNO-np exhibited higher efficiency for generating GSNO from GSH and maintained higher levels of GSNO concentration for longer time (24 h) as compared to SNO-np as well as a previously characterized nitric oxide releasing platform, NO-np (nitric oxide releasing nanoparticles). *In vivo*, intravenous infusion of the NAC-SNO-np and NO-np resulted in sustained decreases in mean arterial pressure, though NAC-SNO-np induced longer vasodilatory effects as compared to the NO-np. Serum chemistries following infusion demonstrated no toxicity in both treatment groups. Together, these data suggest that the NAC-SNO-np represents a novel means to both study the biologic effects of nitrosothiols and effectively capitalize on its therapeutic potential.

Keywords

Nitric Oxide; RSNO; S-nitroso-N-acetyl-cysteine; S-Nitrosoglutathione; Vasodilation; Nanotechnology

© 2012 Published by Elsevier Inc.

Corresponding author: Parimala Nacharaju, Physiology & Biophysics, Albert Einstein College of Medicine, Bronx, NY 10461, Phone: 718-430-8571, parimala.nacharaju@einstein.yu.edu.

¹These authors contributed equally to this work.

Publisher's Disclaimer: This is a PDF file of an unedited manuscript that has been accepted for publication. As a service to our customers we are providing this early version of the manuscript. The manuscript will undergo copyediting, typesetting, and review of the resulting proof before it is published in its final citable form. Please note that during the production process errors may be discovered which could affect the content, and all legal disclaimers that apply to the journal pertain.

Introduction

Nitric oxide (NO) is a small, diatomic gaseous molecule with numerous biological functions. Most notably, it is *the* major endothelial relaxing factor that relaxes smooth muscle by activating guanylate cyclase which, downstream, results in vasodilation via a cyclic guanosine monophosphate-dependent pathway [1; 2; 3]. NO has many other functions that highlight its biomedical importance and therapeutic potential. NO inhibits platelet aggregation [1; 4], plays a major role in macrophage-mediated inflammatory response [1; 5; 6; 7], has antioxidant properties that prevents lipid peroxidation [8; 9], and can function as a signaling molecule in several tissue types including neurons and fibroblasts [1; 10]. The particular physiological consequence of NO is dependent not only on the site/compartiment of production but also on both the rate and amount of NO generated at that location. Despite the many potential therapeutic benefits of supplemental NO, its use as a therapeutic has been limited. This limitation is due in part to the ongoing challenge of creating a practical and economically feasible delivery vehicle for this moderately reactive molecule that is capable of sustained delivery of the appropriate amount of NO to a desired target site [11].

Over the past few decades, several NO-related therapeutics have emerged, though are generally based on complex chemical systems. Unfortunately, these chemical reagents typically cannot spontaneously release NO. Instead, they rely on enzymatic activity to achieve release of NO [12]. These so-called pro-drugs include organonitrates: most notably nitroglycerine and organometallic NO-donors such as sodium nitroprusside. Disadvantages including progressive tachyphylaxis, resulting from depletion of host enzymes required for the generation of NO, potential toxicity from toxic byproducts (e.g., sodium nitroprusside decomposes releasing NO as well as cyanide) [13; 14; 15; 16; 17], and short lived biological impact, all limit their therapeutic efficacy. Gaseous NO, though effective and approved by the FDA for the treatment of pulmonary hypertension [18], is limited due to expense, requirement of delivery via gas tank, and potential toxicity issues from the production of NO₂ [19]. Diazeniumdiolates (commonly referred to as NONOates) are a new class of chemicals which can release NO spontaneously. NONOates contain NO complexed with nucleophiles [20; 21; 22], allowing for controllable rates of NO release via various parameters including pH, temperature and the nature of the nucleophile with which the NO is complexed. Unfortunately, pulmonary and systemic toxicity induced by metabolites of NONOates are a potential issue, as is the formation of met hemoglobin (metHb) limiting RBC oxygen carrying capacity [20].

Recently, novel hydrogel-based nanoparticle platforms have been described capable of releasing internally generated NO at biologically significant levels over sustained time periods [23; 24]. Upon IV infusion, these NO releasing nanoparticles (NO-nps) have been shown to induce long-lived vasodilatory effects in animal models in a dose-dependent manner with much greater efficacy and less metHb build up than NONOates [25]. These infused NO-nps have also been shown to be effective in reversing acellular Hb induced vasoconstriction and in limiting the inflammatory cascade in a hemorrhagic shock model [26]. Topical NO-nps have been effective in treating erectile dysfunction in rat models [27], have potent broad spectrum anti-microbial activity [28; 29] *in vitro*, and accelerate wound and abscess healing in murine models [30; 31; 32; 33].

S-nitrosothiols containing molecules (RSNOs) have come into the biotechnology spotlight recently as molecules that once formed, can extend both the temporal window and functionality for NO associated bioactivity *in vivo* [34; 35; 36; 37; 38; 39]. RSNO half-lives are measured in the minutes to hours [40; 41; 42], whereas free NO has been shown to have a half-life measured in the seconds or less depending on site of production [1]. RSNO-based therapeutics appear to have many very similar physiologic effects as other NO-related therapeutics [34; 43; 44; 45]. They are long-lasting bioactive vasodilators [13; 15; 19; 44] not subject to drug tolerance [13; 14; 15; 19; 46], relax smooth muscle [47], and prevent platelet aggregation [43]. In animal models NAC-SNO reduces plaque buildup secondary to hypercholesterolemia [48], acts as a hypotensive [15], an anti-inflammatory [49], and blocks lipid peroxidation that can limit non-alcoholic fatty liver disease pathology [8]. Much of the biological activity of RSNOs has been attributed to S-transnitrosation, where NO as a nitroso group is transferred from one thiol to another resulting in the nitrosation of reactive thiol containing proteins on cell surfaces, in cells, and in plasma. We have previously demonstrated that when combined with glutathione (GSH), the NO-np effectively and efficiently generate GSNO which, due to its long half-life and ability to transnitrosate, had greater antimicrobial activity than NO-np alone against clinical isolates of gram positive and negative multi drug resistant pathogens [28]. Given both the extended bioactive lifetime of RSNO compared to free NO and the potential differences in target tissues/cells and the success achieved with the NO releasing nanoparticle platform [25; 26; 27; 28; 30; 32; 50], we undertook the production of nanoparticles similar in character and structure, but with the capability of either releasing RSNO species or transferring NO via S-transnitrosation.

In the current study, two novel S-nitrosothiol containing hydrogel-based nanoparticle platforms are presented and compared to the NO-np. The first platform (SNO-np) is an SNO loaded nanoparticle in which the thiols are covalently integrated into the polymeric network of the hydrogel comprising the nanoparticle. The S-nitrosothiol moiety cannot leak out from these particles, and therefore, as a consequence, the particles can only release NO or transfer NO to an external thiol containing molecule with which the SNO-np makes contact. The second platform (NAC-SNO-np) is a nanoparticle with a population of encapsulated NAC-SNO. In this platform, there is also the potential for S-transnitrosation to an external thiol containing molecule. However, with this platform, NAC-SNO as well as NO and other NAC associated products can be released from the nanoparticle at a slow sustained rate. Here, we investigate the efficiency with which each platform generates GSNO, and compare the superior platform to the NO-np in its ability to transnitrosate as represented by vasodilation *in vivo*.

Methods

Materials

TMOS (Tetramethoxysilane), PEG-400, chitosan and all other reagents were purchased from Sigma. MPTS (3-mercaptopropyltrimethoxysilane) was from Gelest Inc.

Synthesis of NO-np/SNO and np/NAC-SNO-np

A TMOS-based sol-gel method was used to prepare all the nanoparticles as described earlier [23]. Briefly, TMOS (3 ml) was hydrolyzed with 1 mM HCl (0.6 ml) by sonication on an ice-bath. The hydrolyzed TMOS (3 ml) was added to a buffer mixture of 1.5 ml of 0.5% chitosan, 1.5 ml of PEG 400 and 24 ml of 50 mM Phosphate, pH 7.4, containing other molecules of interest as shown in Table 1. For NO-np, the cocktail contained nitrite and glucose. For SNO-np, nitrite, glucose and acid-hydrolyzed MPTS were added to the buffer mixture at pH 3. MPTS (2 ml) was hydrolyzed with 1 mM HCl (1 ml) by sonication over ice and 1.5 ml of the hydrolyzed MPTS was used. Hydrolyzed TMOS (3 ml) was then added, which polymerized resulting in a pink, opaque sol-gel. For NAC-SNO-np, N-acetyl-L-cysteine, nitrite and glucose were used at the ratios as shown in Table 1. All the resulting sol-gels were lyophilized and then ball milled in a planetary ball-mill (Fritsch, “Pulverisette 6”) into fine powders.

Np extraction

Nanoparticles (20 mg/ml) were suspended in 0.5 mM diethylenetriaminepenta-acetic acid (DTPA) in phosphate buffered solution (PBS, pH 7.4) and incubated for 1 hour at room temperature on a lab rotator, shielded from light. The mixture was spun down in a micro-centrifuge briefly. A small aliquot of the supernatant (10 μ l) was removed, diluted 100x and analyzed on RPHPLC as described below.

GSNO production

Nps were suspended in glutathione (GSH) solutions prepared in 0.5 mM DTPA/PBS (pH 7.4) at room temperature while mixing on a Lab Rotator shielded from light. At time intervals, aliquots were taken out, 50x diluted and analyzed by RPHPLC.

RPHPLC analysis of the GSNO formation reaction

The reaction products were analyzed by RPHPLC using a Vydac Protein and Peptide C₁₈ analytical column (250 mm \times 4.6 mm) in an isocratic 10mM K₂HPO₄/10mM tetrabutylammonium hydrogen sulfate in 5% acetonitrile running buffer (pH 7.0) at a 0.5 ml/min flow rate and were detected by UV absorbance at 210 nm.

Peak identification and concentration calculation

Peak identities were confirmed by co-elution of known standards from Sigma. GSNO concentrations were determined by peak areas from RPHPLC chromatogram using GSNO standard of known concentration.

Vasodilation experiments

Animal preparation—Investigations were performed in 50–65 g male Golden Syrian Hamsters (Charles River Laboratories, Boston, MA) fitted with a dorsal skinfold chamber window. Animal handling and care followed the NIH Guide for the Care and Use of Laboratory Animals. All experimental protocols were approved by the local animal care committee. The hamster chamber window model is widely used for microvascular studies in

the unanesthetized state, and the complete surgical technique is described in detail elsewhere [51].

Inclusion criteria—Animals were suitable for the experiments if: (1) systemic parameters were within normal range, namely, heart rate (HR) 340 beat/min, mean arterial blood pressure (MAP) 80 mm Hg, systemic Hct 45%, and arterial oxygen partial pressure (P_aO_2) 50 mm Hg; and (2) microscopic examination of the tissue in the chamber observed under 650 \times magnification did not reveal signs of edema or bleeding.

Nanoparticle infusion and monitoring systemic parameters—Animals were infused with nanoparticles suspended in deoxygenated saline. Solutions were infused in a volume of 50 μ l (equivalent to less than 2% of the animals blood volume) via the jugular vein at a rate of 100 μ l/min. MAP and HR were recorded continuously (MP 150, Biopac System; Santa Barbara, CA). Hct was measured from centrifuged arterial blood samples taken in heparinized capillary tubes. Hb content was determined spectrophotometrically from a single drop of blood (B-Hemoglobin, Hemocue, Stockholm, Sweden). The methemoglobin (MetHb) level was measured via the cyanomethemoglobin method [52]. Arterial blood was collected in heparinized glass capillaries and immediately analyzed for P_aO_2 , P_aCO_2 , base excess (BE), and pH (Blood Chemistry Analyzer 248, Bayer, Norwood, MA). The comparatively low P_aO_2 and high P_aCO_2 of these animals are a consequence of their adaptation to a fossorial environment.

Plasma nitrate—Blood samples were collected from carotid artery catheter and centrifuged to separate RBCs and plasma. Plasma proteins were removed by adding equivolume of methanol, and centrifuged at 15000 rpm for 10 min at 4°C. Concentration of nitrate in the supernatant were measured with a NOx analyzer (ENO-20; Eicom, Kyoto, Japan). This analyzer combines Griess method and high-performance liquid chromatography.

Microvascular experimental setup—The unanesthetized animal was placed in a restraining tube with a longitudinal slit from which the window chamber protruded, and then fixed to the microscopic stage of a transillumination intravital microscope (BX51WI, Olympus, New Hyde Park, NY). The animals were given 20 min to adjust to the change in the tube environment before measurements. The tissue image was projected onto a CCD camera (COHU 4815) connected to a video recorder and viewed on a monitor. Measurements were carried out using a 40X (LUMPFL-WIR, numerical aperture 0.8, Olympus) water immersion objective. Microhemodynamic measurements were compared to baseline levels obtained before the experimental procedure. The same vessels and functional capillary fields were followed so that direct comparisons to their baseline levels could be performed allowing for more robust statistics for small sample populations.

Microhemodynamics—Arteriolar and venular blood flow velocities were measured online by using the photodiode cross-correlation method (Photo Diode/Velocity Tracker Model 102B, Vista Electronics, San Diego, CA). The measured centerline velocity was corrected according to vessel size to obtain the mean RBC velocity (V). A video image-shearing method was used to measure vessel diameter (D). Blood flow (Q) was calculated

from the measured values as $Q = \pi \times V (D/2)^2$. Changes in arteriolar and venular diameter from baseline were used as indicators of a change in vascular tone. This calculation assumes a parabolic velocity profile and has been found to be applicable to tubes of 15– 80 μm internal diameters and for Hcts in the range of 6–60%.

Data analysis—Results are presented as mean standard deviation. Data within each group were analyzed using analysis of variance for repeated measurements (ANOVA, Kruskal-Wallis test). When appropriate, post hoc analyses were performed with the Dunn multiple comparison test. All statistics were calculated using GraphPad Prism 4.01 (GraphPad Software, Inc., San Diego, CA). Changes were considered statistically significant if $P < 0.05$.

Results

Preparation of SNO-np

The TMOS-based nanoparticle platform employed to generate the SNO/NAC-SNO-np is based on incorporating the molecules of interest into a sol-gel. Typically the TMOS based sol-gels have sufficiently large “pores/channels” to allow for rapid release of any small molecule. Sustained slow release is achieved by filling the pores with structural biopolymers such as chitosan that can form a strong glass-like hydrogen bonding network with elements of the sol-gel polymeric network. The release of “trapped” small molecules occurs when water enters the nanoparticle and starts to slowly disrupt the hydrogen bonding network allowing sustained release of the molecules [53]. Typically, these sol-gels are prepared by adding hydrolyzed TMOS to 50 mM phosphate buffer, pH 7.4, containing all the components to be enclosed. The basic components of NO-np are nitrite, glucose, chitosan and PEG. The compositions of sol-gel preparations are shown in Table 1. For the synthesis of SNO-np, sulfhydryl groups were incorporated within the gel matrix using MPTS which was covalently incorporated into the sol-gel polymeric network. The amount of MPTS to be used was limited by its interference with the polymerization of TMOS into sol-gel. The amount of TMOS and MPTS used was based on maximizing the amount of incorporated thiols without interfering with the polymerization of TMOS. The nitrite concentration was chosen to generate maximum amount of S-nitrosothiols without leaving an excess of unreacted nitrite. Hydrolyzed MPTS and nitrite were added to a cocktail containing other components of the matrix at pH 3. Immediately, hydrolyzed TMOS was added. A sol-gel is formed as a result of condensation and polymerization reaction of TMOS. The gel immediately turned pink indicating the formation of S-nitrosothiols (SNO). The gel formed in the preparation of NO-np, without the addition of MPTS, was translucent and colorless. The gel was dried and ball milled into particles as described in methods section. The gel/particles were shielded from light, throughout.

Preparation of NAC-SNO-np

NAC-SNO was generated from a mixture of N-acetyl-L-cysteine and nitrite in the preparation of NAC-SNO-np. Three types of NAC-SNO-np were prepared using the same amount of N-acetyl-L-cysteine and varying amounts of nitrite as shown in Table 1. The amount of nitrite used for NAC-SNO-np-2 was comparable to that used for SNO-np. At this concentration of nitrite (0.225 M) and N-acetyl-L-cysteine (0.28 M), all the nitrite was

expected to be utilized in the formation of NAC-SNO. NAC-SNO-np-1 and NAC-SNO-np-3 received the same amount of N-acetyl-L-cysteine (0.28 M) but with 50% and 200% the amount of nitrite used to prepare NAC-SNO-np-2, respectively. Thus NAC-SNO-np-3 was anticipated to release both NAC-SNO and NO.

All the components of the matrix, except hydrolyzed TMOS, were mixed in 50 mM phosphate, pH 7.4. The pH of the mixture dropped to about 3 after adding N-acetyl-L-cysteine. The cocktail instantly turned red due to the formation of NAC-SNO. Hydrolyzed TMOS was added to incorporate NAC-SNO into a sol-gel. A red gel was formed after 24 h incubation that was subsequently dried and ball milled into fine powder. The gel/powder was protected from light and the powder was stored at -80°C for longer life of SNO.

Release of SNO/NAC-SNO nanoparticle payloads

Nanoparticles were suspended in 0.5 mM DTPA/PBS and their released payloads (extracts) were analyzed by RPHPLC (Figure 1A, B, and C). The only detectable species in the extracts of SNO-np was nitrite (Figure 1B). Although an excess of sulfhydryl concentration over nitrite was used in the preparation of SNO-np, significant amount of unreacted nitrite was detected in the extract of SNO-np. However, the size of this nitrite peak was ~30% smaller than the corresponding peak in the extract from NO-np (Figure 1A). This suggests that all the MPTS added was not incorporated into the gel and/or not all of the sulfhydryl groups in the matrix were derivatized to SNO. The ratio of MPTS to TMOS used in the preparation of SNO-np (Table 1) was at the limit in terms of MPTS concentration. Higher amounts of MPTS prevented TMOS polymerization into a sol-gel.

NAC-SNO-np-2 extract contained an insignificant amount of nitrite and no peak corresponding to N-acetyl-L-cysteine was observed (Figure 1C). Additional peaks corresponding to nitrate, NAC-SNO and non-characterized oxidized products of NAC-SNO were detected. RPHPLC analysis of NAC-SNO-np extract monitored at 335 nm displayed only peak 6 (data not shown). This product was determined to be NAC-SNO.

Production of GSNO from a mixture of GSH and SNO/NAC-SNO-np

Nanoparticles were incubated in 0.5 mM DTPA/PBS, pH 7.4, in the presence of GSH and the reaction mixtures were analyzed by RPHPLC (Figure 1 A, B, and C). The reaction mixture of SNO-np (20 mg/ml) and GSH (20 mM) after 1 h incubation demonstrated four peaks in the chromatogram corresponding to unreacted GSH, unreacted nitrite, and the products, GSSG (dimer of GSH) and GSNO (Figure 1B). Similar results were obtained with NO-np (Figure 1A). NAC-SNO-np-2 mixed with GSH also displayed a peak corresponding to GSNO (Figure 1C) that was more prominent than those appearing in the chromatograms of NO-np and SNO-np. Additional peaks representing oxidized products of GSH and NAC-SNO were also present.

The amount of GSNO produced by these particles after 1 h incubation with GSH is shown in Figure 2. SNO-np (3.08 mM) and NO-np (2.74 mM) formed comparable amounts of GSNO. Since SNO-np extract released 30% less nitrite as compared to that of NO-np, transnitrosation by SNO-np must be responsible for at least 30% of total GSNO formation. NAC-SNO-np-2 produced significantly higher amount of GSNO (4.04 mM) as compared to

both NO-np and SNO-np. NAC-SNO-np-2 extract contained negligible amount of nitrite and produced at least 50% more GSNO. Although the same amount of nitrite was used in all these three preparations, NAC-SNO-np-2 produced the largest amount of GSNO, indicating transnitrosation is the major pathway of GSNO formation.

Effect of concentration of NO/SNO-np and GSH on GSNO production

The dose dependent production of GSNO was evaluated varying the concentration of NO/SNO-np at a constant NO/SNO-np and GSH ratio. No GSNO was detected after 1 hour incubation of NO-np or SNO-np at 5 and 10 mg/ml with 5 and 10 mM GSH, respectively (Table 2). However, NAC-SNO-np-2 produced detectable amounts of GSNO at all the concentrations tested. NO-np and SNO-np are capable of generating detectable amount of GSNO only at higher concentrations (20 mg/ml). At higher concentrations (20 mg/ml), the particles were incubated with 20 mM GSH, which reduced the pH of the incubation mixture to approximately 5.0; an acidic pH that may have promoted the GSNO production from NO-np and SNO-np.

Kinetics of GSNO production by NO/SNO-np in the presence of GSH

One of the most pronounced benefits of the hydrogel-based nanoparticle platform used in this study is its capability of maintaining a sustained release of its payload over a number of hours [53]. A time course of the production of GSNO by the SNO/NAC-SNO-np (20 mg/ml) in the presence of GSH (20 mM) was carried out (Figure 3). Maximum levels of GSNO were reached in one hour with NO-np and SNO-np samples, producing 2.74 mM and 3.08 mM, respectively, on average. Interestingly, maximum levels of GSNO were not reached with NAC-SNO-np-2 until the two hour time point, indicating a longer sustained release of NAC-SNO from the particles. The overall amount of GSNO formed by this sample (at 2 hours) was significantly higher (4.19 mM) than that formed by NO-np and SNO-np (Table 3).

The other two formulations of NAC-SNO-np, NAC-SNO-np-1 and NAC-SNO-np-3 also required approximately two hours to release the maximum amounts of enclosed components and form the highest levels of GSNO (Figure 3). The initial rates of GSNO formation as well as the concentrations of GSNO formed were proportional to the initial nitrite concentrations used in the preparation of NAC-SNO-nps. On average NAC-SNO-np-1 through NAC-SNO-np-3 produced 2.01 mM, 4.19 mM, and 7.72 mM GSNO, respectively. The percentage of conversion of nitrite/SNO to GSNO was higher for all the NAC-SNO-np formulations as compared to NO-np or SNO-np (Table 3). The nitrite concentration used in the preparation of NAC-SNO-np-1 was only 50% of that used for NO-np, and more importantly all encapsulated nitrite was utilized for the formation of NAC-SNO. The amount of GSNO formed from NAC-SNO-np-1 was comparable to that formed from NO-np, indicating higher efficiency of S-nitrosation by the SNO motif.

The GSNO concentration in the reaction mixtures of all subtypes of nps started declining after two hours incubation, due to the oxidation of GSNO (Figure 3). After 24 h, the GSNO level in NAC-SNO-np-3 sample decayed the most (92%) and in NAC-SNO-np-2 decayed the least (37%) (Table 3).

Vasodilatory influence of NO-np and NAC-SNO-np-2

NO-np and NAC-SNO-np-2 when infused into hamsters reduced the mean arterial pressure (MAP) and increased the heart rate from baseline (Figure 4). These changes were associated with increased blood vessels diameter (Figure 4). NAC-SNO-np-2 effects in MAP, HR and blood vessels diameter increased in a dose dependent manner (Figure 5), establishing the vasodilatory effect of NAC-SNO-np-2. The magnitudes of these systemic responses to NAC-SNO-np-2 were lower than appreciated with the NO-nps at the lowest concentration tested (10mg/kgbw). However, the effect of the NO-np on MAP began to diminish after two hours following intravenous infusion, while NAC-SNO-np-2 maintained these systemic parameters for a longer period, extending to the duration of the experiment (3 hours). These results demonstrate the long lasting vasodilatory effect of NAC-SNO-np-2. The extended impact is likely due to a greater degree of sustained release of NAC-SNO and/or NO from the particles compared to the release profiles for the other nanoparticle platforms. MetHb concentrations after infusion of NAC-SNO-np-2 were not different compared to NO-np infusion (Table 4). The low levels of MetHb indicate that NAC-SNO-np-2 minimally reduces Hb oxygen carrying capacity and suggest significant potential to increase oxygen transport by increasing blood flow via vasodilation. NAC-SNO-np-2 infusion did not alter serum nitrate levels significantly as compared to the baseline. Additionally, NAC-SNO-np-2 did not affect blood gas parameter in terms of P_aO_2 and P_aCO_2 compared to the baseline. However, NO-np increased the ratio of P_aO_2 to the fraction of inspired oxygen concentration. The release of exogenous NO from the NO-np retains the advantages of NO as a selective pulmonary vasodilator, but at the same time may have the disadvantages of gaseous NO as a therapeutic agent, such as rebound pulmonary hypertension. The minor effects of NAC-SNO-np-2 on the ratio of P_aO_2 to the fraction of inspired oxygen concentration suggest that NAC-SNO-np-2 has limited effects on pulmonary vasculature or preferentially act on the larger conducting airways as compared with the smallest airways (changes of the latter contribute to changes in compliance and gas exchange). Additionally, the limited effect in pulmonary vasculature of NAC-SNO-np may prevent the rebound pulmonary hypertension of free NO therapies.

Discussion

The physiological influence of NO is exerted predominantly through the posttranslational modification and functional regulation of proteins. The interaction of NO with soluble guanylyl cyclase (sGC) and generation of cyclic guanosine monophosphate (cGMP) was described to be the major pathway for the biological effects of NO, earlier [54]. However, evidences are emerging out for cGMP-independent biological influence of NO. The cGMP-independent pathways of NO effects are predicted to be mediated by S-nitrosylation of cysteine thiols of various proteins [55; 56; 57; 58; 59; 60; 61; 62]. Unlike the cGMP-dependent influence of NO that solely relies on protein kinase G, cGMP-independent mechanisms are regulated by S-nitrosylation and denitrosylation of various proteins involved and account for a wide range of NO-mediated functions.

RSNOs are capable of activating sGC and induce accumulation of cGMP [44; 63; 64]. This must be mediated by the NO released from RSNO. However, no co-relation was noticed

between biological effects of RSNOs and the rate of NO released and/or cGMP accumulation, in several studies [45; 63; 65; 66; 67]. RSNOs have also been known to exert biological effects that are independent of sGC, including cGMP-independent vasodilation [56; 68], anti-platelet effects [63; 69] and alterations in enzyme function [55]. Since RSNOs are highly capable transnitrosation agents, cGMP-independent pathways could play major role in the biological effects of these molecules. The lack of co-relation of rates of NO release and biological effects of RSNOs indicate that transfer of other derivatives of NO such as NO⁺ to a protein thiol (S-nitrosylation) may account for several of these actions [70; 71].

S-nitrosation of various proteins has been implicated in physiological processes, including vasodilation, antimicrobial activity and other NO mediated cellular functions [15; 39; 43; 47; 55; 72]. Hypo- or hyper-S-nitrosylation of specific protein targets have been linked to human diseases, such as disorders of the cardiovascular, musculoskeletal and nervous systems [36; 37; 55]. In mouse models, genetic ablation of S-nitrosoglutathione reductase, the enzyme principally responsible for GSNO metabolism, results in enhanced levels of SNO-proteins and significantly attenuates experimental asthma and heart failure models [36]. The Cys-SNO residues identified in *in vivo* proteins/enzymes are located in their catalytic sites and may indicate physiological role for S-nitrosation of the enzymes [36].

RSNO-based therapeutics can be considered more efficient than NO-based therapeutics due to their capacity for long lasting release of NO as well as a more facile transnitrosating capability. In a study involving contraction of isolated arteries, SNO based NO donors have been shown to induce longer-lasting vasodilation than other types of NO donors tested [73]. Unlike many NO-therapeutics based on pro-drugs, RSNO-therapeutics do not need any activation to exhibit transnitrosation activity; it occurs at physiological conditions [34; 43; 45].

NAC-SNO and GSNO have been tested in humans as therapeutics for different clinical conditions. Topical application of NAC-SNO inhibited the contraction frequency and basal pressure of the sphincter of Oddi, and reduced duodenal motility in patients undergoing endoscopic retrograde cholangiopancreatography (ERCP) and biliary manometry [74]. GSNO was shown to exhibit anti-thrombotic effects in healthy human subjects without inducing hypotension when infused at low doses [75; 76]. Intracoronary infusion of GSNO during coronary balloon angioplasty prevented the angioplasty-induced increase in platelet expression of P-selection and glycoprotein IIb/IIIa, without altering blood pressure [77]. GSNO infusion in women with severe pre-eclampsia reduced maternal mean arterial pressure, platelet activation, and uterine artery resistance, without further compromise of fetal Doppler indices [78].

In the present study, the long lasting effect of RSNOs was further extended by enclosing/ conjugating RSNO to sustained-releasing hydrogel-based particles. Although all three formulations, NO-np, SNO-np and NAC-SNO-np-2 are capable of producing GSNO from GSH, NAC-SNO-np-2 was found to be the most potent S-nitrosating agent. NAC-SNO-np-2 is capable of producing greater concentrations of GSNO at lower (physiological) concentrations of GSH and at physiological pH *in vitro*. NAC-SNO-np-2 not only produced

more GSNO but stabilized GSNO for extended periods (at least 24 hours) within medium. This feature is likely to be very significant for GSNO based therapeutic formulations for topical applications (antimicrobial and wound healing etc).

In a Syrian hamster animal model, both NO-np and NAC-SNO-2 induced vasodilation when administered at physiological pH, without adding GSH. NO-np induced vasodilation more rapidly than NAC-SNO-np-2. However, although the vascular impact of NAC-SNO-np-2 was more gradual, it was longer lasting. These results are distinct from the *in vitro* results that only NAC-SNO-np-2 could make significant amount of GSNO at physiological pH and NO-np didn't (5 and 10 mM GSH, Table 2). *In vivo*, decomposition of NO/RSNO drugs is influenced by various factors; reducing agents, metal ions and enzymes [34]. Additionally, multiple pathways (cGMP-dependent and cGMP-independent) are operative in biological effects of NO/RSNO. These factors can contribute to the differential influence of NO and RSNO based drugs.

The longer vasodilation effects induced by NAC-SNO-np-2 as compared to NO-np are consistent with the previous observations on the differential influence of SNO-based and NO-based NO donors on the relaxation of isolated arteries [73]. Isolated arteries exposed to SNO-based drugs and subsequently washed were found to be less contracted in response to norepinephrine as compared to controls; NO-based drugs however could not confer similar protection from norepinephrine induced contraction. S-nitrosation of arterial tissue proteins by SNO-based drugs was suggested as a possible source of NO storage to induce long lasting vasodilation.

In addition, NAC-SNO has been shown to induce hypotension more effectively than sodium nitroprusside (SNP) in normal and acute hypertension induced rats [15]. SNP is currently in use to treat malignant hypertension in emergency settings and cardiac failure [79; 80]. The vascular effect of NAC-SNO (~9 min) was much longer than that of SNP (~1 min). NAC-SNO-np-2 in the current study maintained a decrease in MAP in hamsters for several hours, establishing the enhanced benefits of nanoparticle based formulation for sustained release of NAC-SNO for therapeutic applications.

We have formulated three types of NAC-SNO-np using different concentrations of nitrite and a constant amount of N-acetyl-L-cysteine (Table 1) to determine the contribution of NO/SNO towards S-nitrosation. Based on the total nitrite/SNO concentrations contained, all the three formulations of NAC-SNO-np generated more GSNO as compared to NO-np (Table 3). Importantly, although NAC-SNO-np-1 was made with only 50% amount of nitrite as compared to NO-np and was not found to release any unreacted nitrite, these particles generated analogous concentrations of GSNO to NO-np. These results clearly indicate that S-transnitrosation by NAC-SNO is a more efficient approach to form RSNO or S-nitrosothiols on proteins than simply by nitrite/NO mediated S-nitrosylation.

The composition of NAC-SNO-np-3 is similar to 1:1 combination of NAC-SNO-np-2 (in terms of SNO) and NO-np (in terms of NO). Along these lines, the amount of GSNO generated by NAC-SNO-np-3 was also comparable to the sum of that generated by the other two formulations. NAC-SNO-np-3 is expected to exert vasodilatory effects *in vivo* along the

lines of a combination of the effects seen with NO-np (immediate effect) and NAC-SNO-np-2 (long lasting effect). Additionally, NAC-SNO-np-3 is advantageous over a combination of NO-np and NAC-SNO-np-2 since it would use only 50% of the particles. The amount of particles that must be infused is a critical factor for *in vivo* applications.

Although NAC-SNO-np-3 produced more GSNO than NAC-SNO-np-2, at the end of 24 h NAC-SNO-np-2 retained more GSNO than NAC-SNO-np-3. This feature makes NAC-SNO-np-2 a practical NO/GSNO based therapeutic for topical applications such as wound healing, antimicrobial, and erectile dysfunction treatment.

In the present studies, the formation of GSNO from GSH was used as a model reaction to evaluate the transnitrosating efficiency of the nanoparticle formulations. We propose that these relative efficiencies of the formulations may be extended to the transnitrosation of protein thiols. NAC-SNO-np formulations can make efficient therapeutics in physiological processes involving S-nitrosation of protein thiols. In addition to NAC-SNO, other RSNOs such as SNO-captopril can also make a good candidate for nanoparticle based delivery. Captopril is an angiotensin-converting enzyme (ACE) inhibitor and is used for hypertension. SNO-captopril is a transnitrosating agent and [81; 82] has been shown to control acute and chronic hypertensive effects more efficiently than captopril in rats [83; 84].

The hydrogel-based nanoparticle platform that has been employed in the present study is comprised of N-acetyl-L-cysteine, nitrite, glucose, chitosan, PEG 400 and a silica backbone, all of which have been shown previously to be non-toxic [25]. The control nanoparticles (comprising of TMOS, chitosan and PEG 400) did not induce adverse effects, except that a decrease in the number of capillaries perfused and an increase in leukocyte rolling and immobilization in the microcirculation were observed. The NO released by the NO-np prevents the inflammatory response observed after infusion of control-np. RSNO based therapeutics do not appear to induce tolerance in animals. However, the stability of RSNOs *in vivo* may be influenced by metal ions, reducing agent such as ascorbic acid and other thiols ultimately limiting their therapeutic efficacy [43]. Nanoparticle based sustained release of RSNOs may be an approach to enhance their stability *in vivo*, importantly when used in circulation. The presented NAC-SNO-np represents a novel example of such a therapeutic for systemic and topical applications.

Conclusions

In the present study, we have generated hydrogel based S-nitroso-N-acetyl cysteine releasing nanoparticles (NAC-SNO-np). NAC-SNO-np exhibited higher efficiency for generating GSNO from GSH and maintained higher levels of GSNO than previously characterized nitric oxide releasing platform, NO-np. Intravenous infusion of the NAC-SNO-np into hamsters resulted in sustained reduction in mean arterial pressure, induced longer vasodilatory effects as compared to the NO-np. We propose that nanoparticle based sustained release of RSNOs is an approach to enhance their stability in circulation and achieve long lasting therapeutic effects.

Abbreviations

NO	nitric oxide
GSH	glutathione
GSNO	S-nitrosoglutathione
RSNO	S-nitrosothiols containing molecules
NO-np	nitric oxide releasing nanoparticles
SNO-np	S-nitrosothiol loaded nanoparticles
NAC-SNO-np	S-nitroso-N-acetylcysteine releasing nanoparticles
TMOS	Tetramethoxysilane
MPTS	3-mercaptopropyltrimethoxysilane
RPHPLC	reverse phase high performance liquid chromatography
PBS	phosphate buffered saline
DTPA	diethylenetriaminepenta-acetic acid
MAP	mean arterial blood pressure
HR	heart rate
MetHb	methemoglobin
RBCs	red blood cells
BE	base excess

References

1. Butler AR, Flitney FW, Williams DL. NO, nitrosonium ions, nitroxide ions, nitrosothiols and iron-nitrosyls in biology: a chemist's perspective. *Trends Pharmacol Sci.* 1995; 16:18–22. [PubMed: 7732599]
2. Hanafy KA, Krumenacker JS, Murad F. NO, nitrotyrosine, and cyclic GMP in signal transduction. *Med Sci Monit.* 2001; 7:801–19. [PubMed: 11433215]
3. McDonald LJ, Murad F. Nitric oxide and cyclic GMP signaling. *Proc Soc Exp Biol Med.* 1996; 211:1–6. [PubMed: 8594612]
4. Radomski MW, Palmer RM, Moncada S. Comparative pharmacology of endothelium-derived relaxing factor, nitric oxide and prostacyclin in platelets. *Br J Pharmacol.* 1987; 92:181–7. [PubMed: 3311265]
5. Marletta MA, Yoon PS, Iyengar R, Leaf CD, Wishnok JS. Macrophage oxidation of L-arginine to nitrite and nitrate: nitric oxide is an intermediate. *Biochemistry.* 1988; 27:8706–11. [PubMed: 3242600]
6. Hibbs JB Jr, Taintor RR, Vavrin Z, Rachlin EM. Nitric oxide: a cytotoxic activated macrophage effector molecule. *Biochem Biophys Res Commun.* 1988; 157:87–94. [PubMed: 3196352]
7. Stuehr DJ, Gross SS, Sakuma I, Levi R, Nathan CF. Activated murine macrophages secrete a metabolite of arginine with the bioactivity of endothelium-derived relaxing factor and the chemical reactivity of nitric oxide. *J Exp Med.* 1989; 169:1011–20. [PubMed: 2784476]
8. de Oliveira CP, Simplicio FI, de Lima VM, Yuahasi K, Lopasso FP, Alves VA, Abdalla DS, Carrilho FJ, Laurindo FR, de Oliveira MG. Oral administration of S-nitroso-N-acetylcysteine

- prevents the onset of non alcoholic fatty liver disease in rats. *World J Gastroenterol.* 2006; 12:1905–11. [PubMed: 16609997]
9. Rubbo H, Darley-Usmar V, Freeman BA. Nitric oxide regulation of tissue free radical injury. *Chem Res Toxicol.* 1996; 9:809–20. [PubMed: 8828915]
 10. Jaffrey SR, Snyder SH. Nitric oxide: a neural messenger. *Annu Rev Cell Dev Biol.* 1995; 11:417–40. [PubMed: 8689564]
 11. Friedman A, Friedman J. New biomaterials for the sustained release of nitric oxide: past, present and future. *Expert Opinion on Drug Delivery.* 2009; 6:1113–1122. [PubMed: 19663720]
 12. Thatcher GR. An introduction to NO-related therapeutic agents. *Curr Top Med Chem.* 2005; 5:597–601. [PubMed: 16101422]
 13. Henry PJ, Drummer OH, Horowitz JD. S-nitrosothiols as vasodilators: implications regarding tolerance to nitric oxide-containing vasodilators. *Br J Pharmacol.* 1989; 98:757–66. [PubMed: 2511992]
 14. Kowaluk EA, Poliszczuk R, Fung HL. Tolerance to relaxation in rat aorta: comparison of an S-nitrosothiol with nitroglycerin. *Eur J Pharmacol.* 1987; 144:379–83. [PubMed: 3126076]
 15. Ricardo KF, Shishido SM, de Oliveira MG, Krieger MH. Characterization of the hypotensive effect of S-nitroso-N-acetylcysteine in normotensive and hypertensive conscious rats. *Nitric Oxide.* 2002; 7:57–66. [PubMed: 12175821]
 16. Bates JN, Baker MT, Guerra R Jr, Harrison DG. Nitric oxide generation from nitroprusside by vascular tissue. Evidence that reduction of the nitroprusside anion and cyanide loss are required. *Biochem Pharmacol.* 1991; 42(Suppl):S157–65. [PubMed: 1768273]
 17. Butler AR, Glidewell C, McGinnis J, Bisset WI. Further investigations regarding the toxicity of sodium nitroprusside. *Clin Chem.* 1987; 33:490–2. [PubMed: 3829378]
 18. Hagan G, Pepke-Zaba J. Pulmonary hypertension, nitric oxide and nitric oxide-releasing compounds. *Expert Rev Respir Med.* 5:163–71. [PubMed: 21510727]
 19. Butler AR, Rhodes P. Chemistry, analysis, and biological roles of S-nitrosothiols. *Anal Biochem.* 1997; 249:1–9. [PubMed: 9193701]
 20. Lam CF, Sviri S, Ilett KF, van Heerden PV. Inhaled diazeniumdiolates (NONOates) as selective pulmonary vasodilators. *Expert Opin Investig Drugs.* 2002; 11:897–909.
 21. Maragos CM, Morley D, Wink DA, Dunams TM, Saavedra JE, Hoffman A, Bove AA, Isaac L, Hrabie JA, Keefer LK. Complexes of .NO with nucleophiles as agents for the controlled biological release of nitric oxide. Vasorelaxant effects. *J Med Chem.* 1991; 34:3242–7. [PubMed: 1956043]
 22. Maragos CM, Wang JM, Hrabie JA, Oppenheim JJ, Keefer LK. Nitric oxide/nucleophile complexes inhibit the in vitro proliferation of A375 melanoma cells via nitric oxide release. *Cancer Res.* 1993; 53:564–8. [PubMed: 8425188]
 23. Friedman AJ, Han G, Navati MS, Chacko M, Gunther L, Alfieri A, Friedman JM. Sustained release nitric oxide releasing nanoparticles: characterization of a novel delivery platform based on nitrite containing hydrogel/glass composites. *Nitric Oxide.* 2008; 19:12–20. [PubMed: 18457680]
 24. Han G, Friedman AJ, Friedman JM. Nitric oxide releasing nanoparticle synthesis and characterization. *Methods Mol Biol.* 2011; 704:187–95. [PubMed: 21161638]
 25. Cabrales P, Han G, Roche C, Nacharaju P, Friedman AJ, Friedman JM. Sustained release nitric oxide from long-lived circulating nanoparticles. *Free Radic Biol Med.* 2010; 49:530–8. [PubMed: 20460149]
 26. Cabrales P, Han G, Nacharaju P, Friedman AJ, Friedman JM. Reversal of hemoglobin-induced vasoconstriction with sustained release of nitric oxide. *Am J Physiol Heart Circ Physiol.* 2011; 300:H49–56. [PubMed: 21057038]
 27. Han G, Tar M, Kuppam DS, Friedman A, Melman A, Friedman J, Davies KP. Nanoparticles as a novel delivery vehicle for therapeutics targeting erectile dysfunction. *J Sex Med.* 2010; 7:224–33. [PubMed: 19765204]
 28. Friedman A, Blecher K, Sanchez D, Tuckman-Vernon C, Gialanella P, Friedman JM, Martinez LR, Nosanchuk JD. Susceptibility of Gram-positive and -negative bacteria to novel nitric oxide-releasing nanoparticle technology. *Virulence.* 2011; 2:217–21. [PubMed: 21577055]
 29. Friedman AJ, Blecher K, Schairer D, Tuckman-Vernon C, Nacharaju P, Sanchez D, Gialanella P, Martinez LR, Friedman JM, Nosanchuk JD. Improved antimicrobial efficacy with nitric oxide

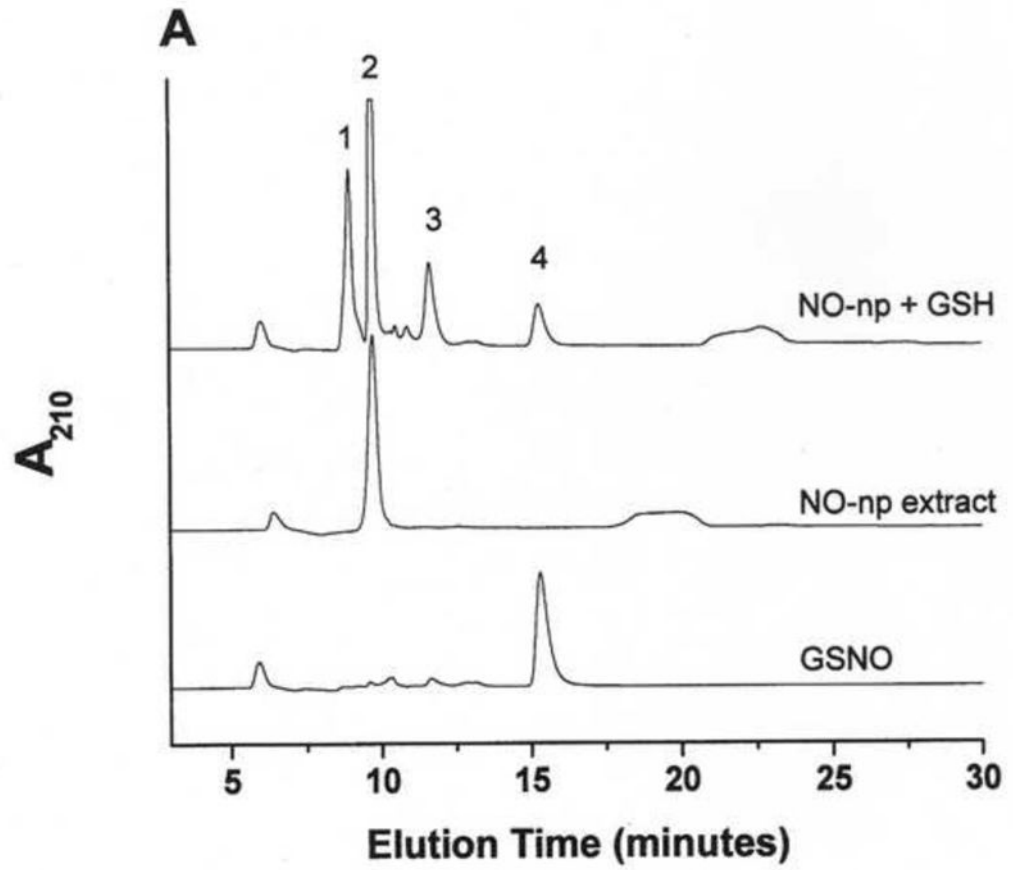
- releasing nanoparticle generated S-nitrosoglutathione. *Nitric Oxide*. 2011; 25:381–6. [PubMed: 21946032]
30. Han G, Martinez LR, Mihi MR, Friedman AJ, Friedman JM, Nosanchuk JD. Nitric oxide releasing nanoparticles are therapeutic for *Staphylococcus aureus* abscesses in a murine model of infection. *PLoS One*. 2009; 4:e7804. [PubMed: 19915659]
 31. Mihi MR, Sandkovsky U, Han G, Friedman JM, Nosanchuk JD, Martinez LR. The use of nitric oxide releasing nanoparticles as a treatment against *Acinetobacter baumannii* in wound infections. *Virulence*. 2010; 1:62–7. [PubMed: 21178416]
 32. Martinez LR, Han G, Chacko M, Mihi MR, Jacobson M, Gialanella P, Friedman AJ, Nosanchuk JD, Friedman JM. Antimicrobial and healing efficacy of sustained release nitric oxide nanoparticles against *Staphylococcus aureus* skin infection. *J Invest Dermatol*. 2009; 129:2463–9. [PubMed: 19387479]
 33. Schairer D, Martinez L, Blecher K, Chouake J, Nacharaju P, Gialanella P, Friedman JM, Nosanchuk J, Friedman A. Nitric oxide nanoparticles: Pre-clinical utility as a therapeutic for intramuscular abscesses. *Virulence*. 2012; 3
 34. Al-Sa'doni HH, Ferro A. S-nitrosothiols as nitric oxide-donors: chemistry, biology and possible future therapeutic applications. *Curr Med Chem*. 2004; 11:2679–90. [PubMed: 15544469]
 35. Diesen DL, Hess DT, Stamler JS. Hypoxic vasodilation by red blood cells: evidence for an S-nitrosothiol-based signal. *Circ Res*. 2008; 103:545–53. [PubMed: 18658051]
 36. Foster MW, Hess DT, Stamler JS. Protein S-nitrosylation in health and disease: a current perspective. *Trends Mol Med*. 2009; 15:391–404. [PubMed: 19726230]
 37. Foster MW, McMahon TJ, Stamler JS. S-nitrosylation in health and disease. *Trends Mol Med*. 2003; 9:160–8. [PubMed: 12727142]
 38. Giustarini D, Milzani A, Colombo R, Dalle-Donne I, Rossi R. Nitric oxide and S-nitrosothiols in human blood. *Clin Chim Acta*. 2003; 330:85–98. [PubMed: 12636927]
 39. Stamler JS, Simon DI, Osborne JA, Mullins ME, Jaraki O, Michel T, Singel DJ, Loscalzo J. S-nitrosylation of proteins with nitric oxide: synthesis and characterization of biologically active compounds. *Proc Natl Acad Sci U S A*. 1992; 89:444–8. [PubMed: 1346070]
 40. Hornyak I, Marosi K, Kiss L, Grof P, Lacza Z. Increased stability of S-nitrosothiol solutions via pH modulations. *Free Radic Res*.
 41. Hu TM, Chou TC. The kinetics of thiol-mediated decomposition of S-nitrosothiols. *Aaps J*. 2006; 8:E485–92. [PubMed: 17025266]
 42. Grossi L, Montevecchi PC. A kinetic study of S-nitrosothiol decomposition. *Chemistry*. 2002; 8:380–7. [PubMed: 11843150]
 43. Richardson G, Benjamin N. Potential therapeutic uses for S-nitrosothiols. *Clin Sci (Lond)*. 2002; 102:99–105. [PubMed: 11749666]
 44. Mellion BT, Ignarro LJ, Myers CB, Ohlstein EH, Ballot BA, Hyman AL, Kadowitz PJ. Inhibition of human platelet aggregation by S-nitrosothiols. Heme-dependent activation of soluble guanylate cyclase and stimulation of cyclic GMP accumulation. *Mol Pharmacol*. 1983; 23:653–64. [PubMed: 6135148]
 45. Al-Sa'doni H, Ferro A. S-Nitrosothiols: a class of nitric oxide-donor drugs. *Clin Sci (Lond)*. 2000; 98:507–20. [PubMed: 10781381]
 46. Al-Sa'doni HH, Khan IY, Poston L, Fisher I, Ferro A. A novel family of S-nitrosothiols: chemical synthesis and biological actions. *Nitric Oxide*. 2000; 4:550–60. [PubMed: 11139363]
 47. Ignarro LJ, Lippton H, Edwards JC, Baricos WH, Hyman AL, Kadowitz PJ, Gruetter CA. Mechanism of vascular smooth muscle relaxation by organic nitrates, nitrites, nitroprusside and nitric oxide: evidence for the involvement of S-nitrosothiols as active intermediates. *J Pharmacol Exp Ther*. 1981; 218:739–49. [PubMed: 6115052]
 48. Krieger MH, Santos KF, Shishido SM, Wanschel AC, Estrela HF, Santos L, De Oliveira MG, Franchini KG, Spadari-Bratfisch RC, Laurindo FR. Antiatherogenic effects of S-nitroso-N-acetylcysteine in hypercholesterolemic LDL receptor knockout mice. *Nitric Oxide*. 2006; 14:12–20. [PubMed: 16198610]
 49. Garcia JA, dos Santos L, Moura AL, Ricardo KF, Wanschel AC, Shishido SM, Spadari-Bratfisch RC, de Souza HP, Krieger MH. S-nitroso-N-acetylcysteine (SNAC) prevents myocardial

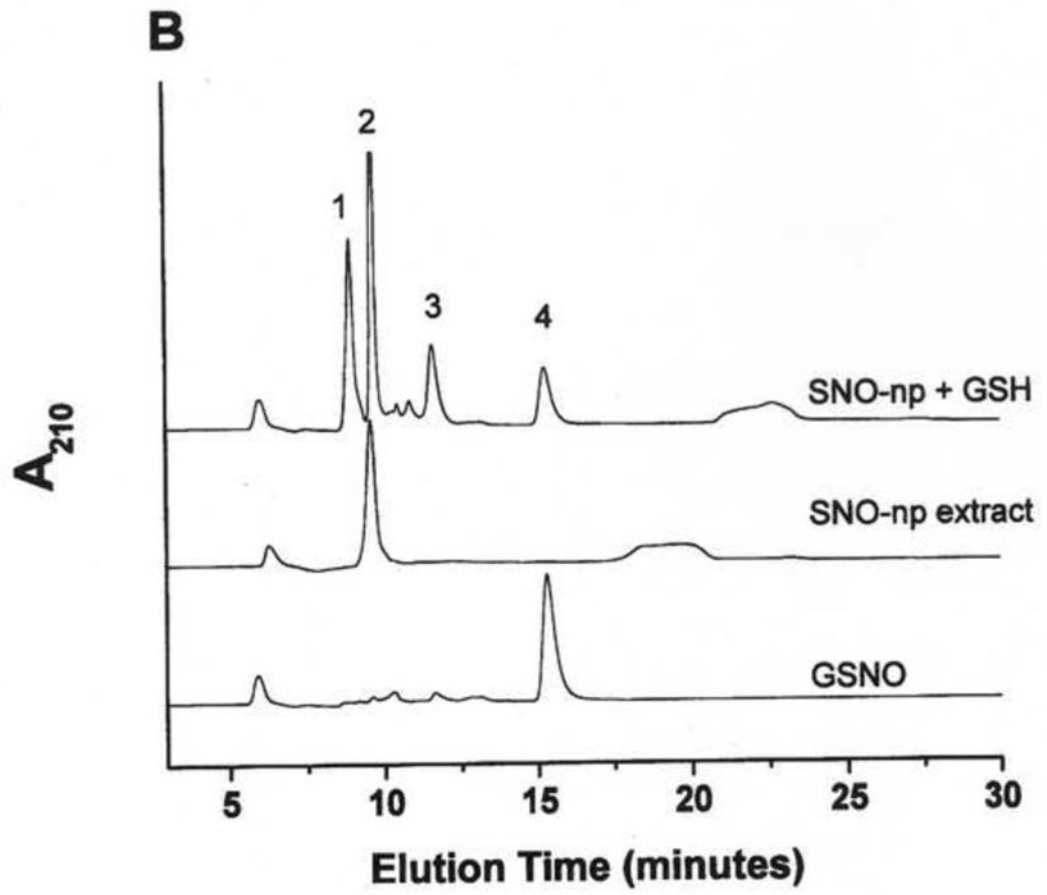
- alterations in hypercholesterolemic LDL receptor knockout mice by antiinflammatory action. *J Cardiovasc Pharmacol.* 2008; 51:78–85. [PubMed: 18209572]
50. Nacharaju P, Friedman AJ, Friedman JM, Cabrales P. Exogenous nitric oxide prevents cardiovascular collapse during hemorrhagic shock. *Resuscitation.* 2011; 82:607–13. [PubMed: 21342744]
51. Colantuoni A, Bertuglia S, Intaglietta M. Quantitation of rhythmic diameter changes in arterial microcirculation. *Am J Physiol.* 1984; 246:H508–H517. [PubMed: 6720909]
52. Sakata M, Yoshida A, Haga M. Methemoglobin in blood as determined by double-wavelength spectrophotometry. *Clin Chem.* 1982; 28:508–11. [PubMed: 7067094]
53. Friedman AJ, Han G, Navati MS, Chacko M, Gunther L, Alfieri A, Friedman JM. Sustained release nitric oxide releasing nanoparticles: Characterization of a novel delivery platform based on nitrite containing hydrogel/glass composites. *Nitric Oxide-Biology and Chemistry.* 2008; 19:12–20.
54. Murad F. Cyclic guanosine monophosphate as a mediator of vasodilation. *J Clin Invest.* 1986; 78:1–5. [PubMed: 2873150]
55. Lima B, Forrester MT, Hess DT, Stamler JS. S-nitrosylation in cardiovascular signaling. *Circ Res.* 2010; 106:633–46. [PubMed: 20203313]
56. Wanstall JC, Homer KL, Doggrel SA. Evidence for, and importance of, cGMP-independent mechanisms with NO and NO donors on blood vessels and platelets. *Curr Vasc Pharmacol.* 2005; 3:41–53. [PubMed: 15638781]
57. Hamad AM, Clayton A, Islam B, Knox AJ. Guanylyl cyclases, nitric oxide, natriuretic peptides, and airway smooth muscle function. *Am J Physiol Lung Cell Mol Physiol.* 2003; 285:L973–83. [PubMed: 14551038]
58. Ahern GP, Klyachko VA, Jackson MB. cGMP and S-nitrosylation: two routes for modulation of neuronal excitability by NO. *Trends Neurosci.* 2002; 25:510–7. [PubMed: 12220879]
59. Brune B, Mohr S, Messmer UK. Protein thiol modification and apoptotic cell death as cGMP-independent nitric oxide (NO) signaling pathways. *Rev Physiol Biochem Pharmacol.* 1996; 127:1–30. [PubMed: 8533007]
60. Murad F. Nitric oxide and cyclic guanosine monophosphate signaling in the eye. *Can J Ophthalmol.* 2008; 43:291–4. [PubMed: 18443613]
61. Boerrigter G, Lapp H, Burnett JC. Modulation of cGMP in heart failure: a new therapeutic paradigm. *Handb Exp Pharmacol.* 2009:485–506. [PubMed: 19089342]
62. Hogg N. The biochemistry and physiology of S-nitrosothiols. *Annu Rev Pharmacol Toxicol.* 2002; 42:585–600. [PubMed: 11807184]
63. Gordge MP, Hothersall JS, Noronha-Dutra AA. Evidence for a cyclic GMP-independent mechanism in the anti-platelet action of S-nitrosoglutathione. *Br J Pharmacol.* 1998; 124:141–8. [PubMed: 9630353]
64. Severina IS, Bussygina OG, Pyatakova NV, Malenkova IV, Vanin AF. Activation of soluble guanylate cyclase by NO donors--S-nitrosothiols, and dinitrosyl-iron complexes with thiol-containing ligands. *Nitric Oxide.* 2003; 8:155–63. [PubMed: 12826064]
65. Butler AR, Al-Sa'doni HH, Megson IL, Flitney FW. Synthesis, decomposition, and vasodilator action of some new S-nitrosated dipeptides. *Nitric Oxide.* 1998; 2:193–202. [PubMed: 9731637]
66. Kowaluk EA, Fung HL. Spontaneous liberation of nitric oxide cannot account for in vitro vascular relaxation by S-nitrosothiols. *J Pharmacol Exp Ther.* 1990; 255:1256–64. [PubMed: 2175799]
67. Mathews WR, Kerr SW. Biological activity of S-nitrosothiols: the role of nitric oxide. *J Pharmacol Exp Ther.* 1993; 267:1529–37. [PubMed: 7903392]
68. Fernandes VS, Martinez-Saenz A, Recio P, Ribeiro AS, Sanchez A, Martinez MP, Martinez AC, Garcia-Sacristan A, Orensanz LM, Prieto D, Hernandez M. Mechanisms involved in the nitric oxide-induced vasorelaxation in porcine prostatic small arteries. *Naunyn Schmiedebergs Arch Pharmacol.* 2011; 384:245–53. [PubMed: 21748357]
69. Priora R, Margaritis A, Frosali S, Coppo L, Summa D, Di Giuseppe D, Aldinucci C, Pessina G, Di Stefano A, Di Simplicio P. In vitro inhibition of human and rat platelets by NO donors, nitrosoglutathione, sodium nitroprusside and SIN-1, through activation of cGMP-independent pathways. *Pharmacol Res.* 2011; 64:289–97. [PubMed: 21539916]

70. Stamler JS. S-nitrosothiols and the bioregulatory actions of nitrogen oxides through reactions with thiol groups. *Curr Top Microbiol Immunol.* 1995; 196:19–36. [PubMed: 7634823]
71. Arnelle DR, Stamler JS. NO⁺, NO, and NO⁻ donation by S-nitrosothiols: implications for regulation of physiological functions by S-nitrosylation and acceleration of disulfide formation. *Arch Biochem Biophys.* 1995; 318:279–85. [PubMed: 7733655]
72. Hess DT, Matsumoto A, Kim SO, Marshall HE, Stamler JS. Protein S-nitrosylation: purview and parameters. *Nat Rev Mol Cell Biol.* 2005; 6:150–66. [PubMed: 15688001]
73. Alencar JL, Lobysheva I, Chalupsky K, Geffard M, Nepveu F, Stoclet JC, Muller B. S-nitrosating nitric oxide donors induce long-lasting inhibition of contraction in isolated arteries. *J Pharmacol Exp Ther.* 2003; 307:152–9. [PubMed: 12954813]
74. Slivka A, Chuttani R, Carr-Locke DL, Kobzik L, Bredt DS, Loscalzo J, Stamler JS. Inhibition of sphincter of Oddi function by the nitric oxide carrier S-nitroso-N-acetylcysteine in rabbits and humans. *J Clin Invest.* 1994; 94:1792–8. [PubMed: 7525649]
75. de Belder AJ, MacAllister R, Radomski MW, Moncada S, Vallance PJ. Effects of S-nitroso-glutathione in the human forearm circulation: evidence for selective inhibition of platelet activation. *Cardiovasc Res.* 1994; 28:691–4. [PubMed: 8025915]
76. Ramsay B, Radomski M, De Belder A, Martin JF, Lopez-Jaramillo P. Systemic effects of S-nitroso-glutathione in the human following intravenous infusion. *Br J Clin Pharmacol.* 1995; 40:101–2. [PubMed: 8527258]
77. Langford EJ, Brown AS, Wainwright RJ, de Belder AJ, Thomas MR, Smith RE, Radomski MW, Martin JF, Moncada S. Inhibition of platelet activity by S-nitrosoglutathione during coronary angioplasty. *Lancet.* 1994; 344:1458–60. [PubMed: 7526102]
78. Lees C, Langford E, Brown AS, de Belder A, Pickles A, Martin JF, Campbell S. The effects of S-nitrosoglutathione on platelet activation, hypertension, and uterine and fetal Doppler in severe preeclampsia. *Obstet Gynecol.* 1996; 88:14–9. [PubMed: 8684748]
79. Elkayam U, Janmohamed M, Habib M, Hatamizadeh P. Vasodilators in the management of acute heart failure. *Crit Care Med.* 2008; 36:S95–105. [PubMed: 18158484]
80. Kirk JD, Parissis JT, Filippatos G. Pharmacologic stabilization and management of acute heart failure syndromes in the emergency department. *Heart Fail Clin.* 2009; 5:43–54. vi. [PubMed: 19026385]
81. Park JW. Dual role of S-nitrosocaptopril as an inhibitor of angiotensin-converting enzyme and a nitroso group carrier. *Biochem Biophys Res Commun.* 1992; 189:206–10. [PubMed: 1449475]
82. Dasgupta TP, Aquart DV. Transfer of nitric oxide from nitrovasodilators to free thiols--evidence of two distinct stages. *Biochem Biophys Res Commun.* 2005; 335:730–3. [PubMed: 16095564]
83. Jia L, Blantz RC. The effects of S-nitrosocaptopril on renal filtration and blood pressure in rats. *Eur J Pharmacol.* 1998; 354:33–41. [PubMed: 9726628]
84. Tsui DY, Gambino A, Wanstall JC. S-nitrosocaptopril: acute in-vivo pulmonary vasodepressor effects in pulmonary hypertensive rats. *J Pharm Pharmacol.* 2003; 55:1121–5. [PubMed: 12956902]

Highlights

- Novel hydrogel based RSNO containing nanoparticle platforms.
- S-nitroso-N-acetyl cysteine releasing nanoparticles (NAC-SNO-np)
- NAC-SNO-np efficiently generates GSNO from GSH.
- NAC-SNO-np acts as a long lived vasodilator.





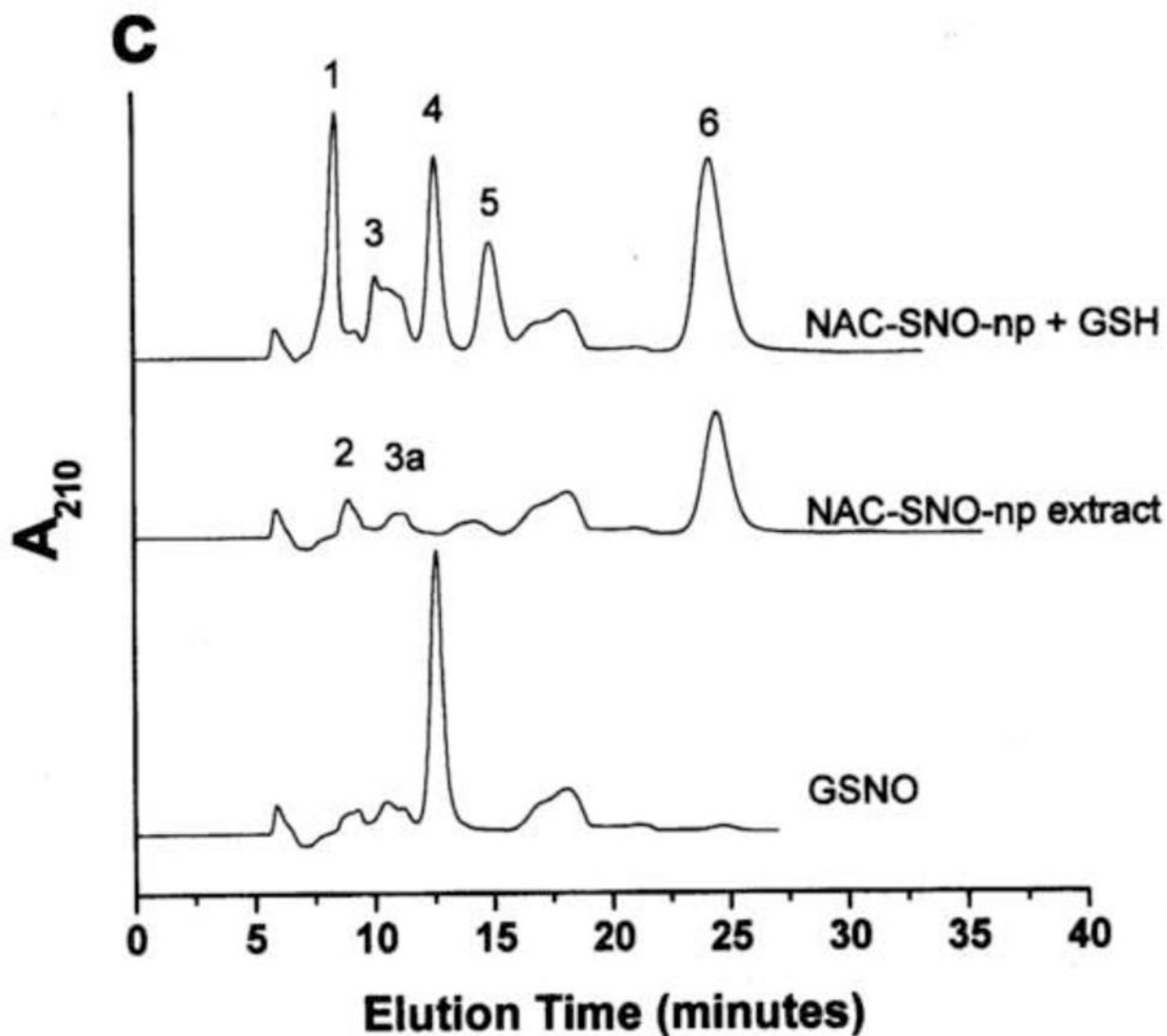


Figure 1. GSNO production from nanoparticles

NO-np (A), SNO-np (B), and NAC-SNO-np-2 (C) were incubated at 20 mg/ml in 0.5 mM DTPA/PBS, pH 7.4 for 1 hour at room temperature shielded from light in the absence and presence of GSH (20 mM) while mixing on a lab rotator. Supernatants were diluted (100x for extracts and 50x for GSH-reaction mixtures) and analyzed by RPHPLC as described in the text. GSH-reaction mixtures of all the particles displayed a peak corresponding to GSNO, which was absent in the respective extracts (in the absence of GSH). Peaks identities are as follows: 1 = GSH, 2 = nitrite, 3 = GSSG, 3a = nitrate, 4 = GSNO, 5 = non-characterized oxidized product of NAC-SNO, 6 = NAC-SNO.

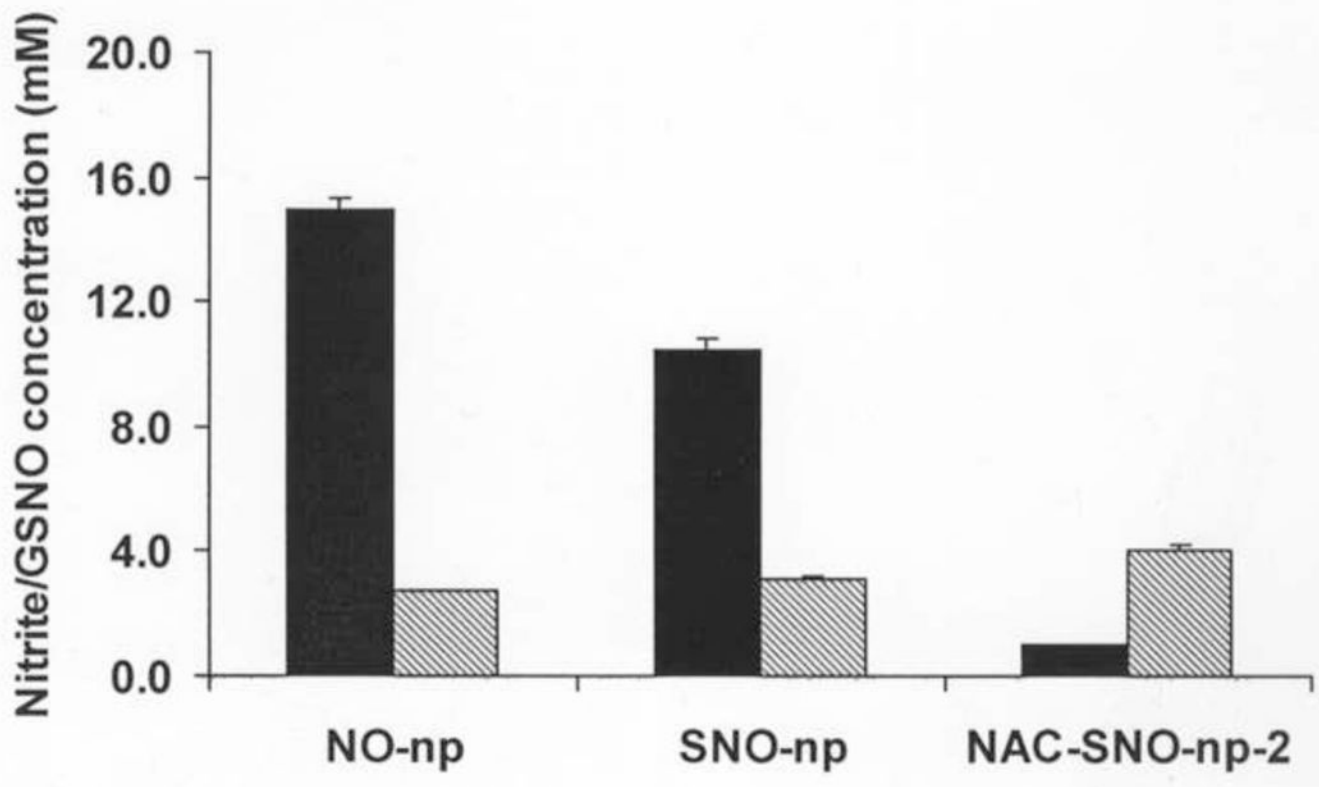


Figure 2. Comparison of GSNO production from nanoparticles

Amount of nitrite released (filled bars) or GSNO formed (striped bars) when nanoparticles (20 mg/ml) were incubated in DTPA/PBS (pH 7.4) at room temperature for 1 hour in the absence or presence of GSH (20 mM), respectively. NO-np released the highest amount of nitrite and formed the least amount of GSNO with GSH. These results were opposite with NAC-SNO-np-2, indicating higher efficiency of NAC-SNO to form GSNO by S-transnitrosation. The results are the averages of duplicate experiments.

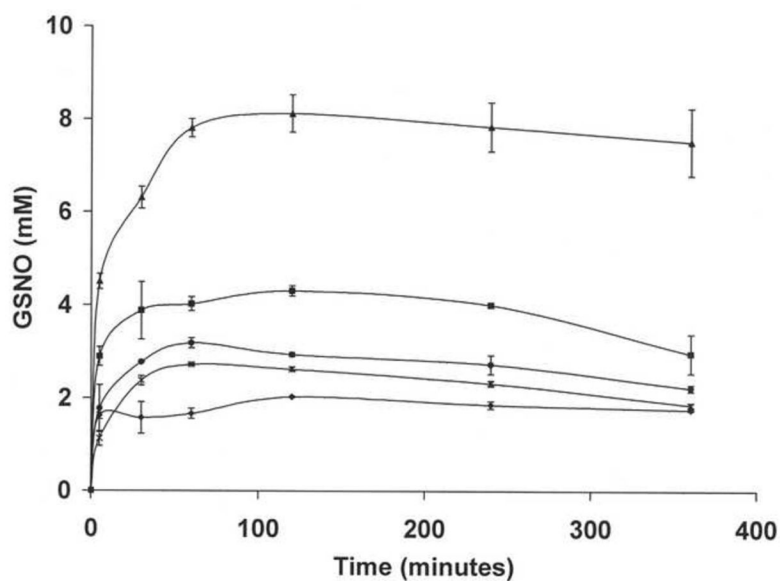


Figure 3. Time course of GSNO production from a mixture of nanoparticles and GSH NO-np (*), SNO-np (●), NAC-SNO-np-1 (◆), NAC-SNO-np-2 (■), and NAC-SNO-np-3 (▲) (20 mg/ml) were incubated with GSH (20 mM) in 0.5 mM DTPA/PBS, pH 7.4, at room temperature. Aliquots were taken at time intervals, 50x diluted and analyzed by RPHPLC as described in methods. GSNO concentrations were calculated from the peak areas. Values are the averages of duplicate experiments. In spite of using the same amount of nitrite, NAC-SNO-np-2 formed more GSNO and at a higher rate than NO-np and SNO-np. The rate and amount of GSNO formed from the three formulations of NAC-SNO-np were proportional to the amount of nitrite used in the preparation of these particles. These results demonstrate the highest S-nitrosation efficiency of NAC-SNO-np.

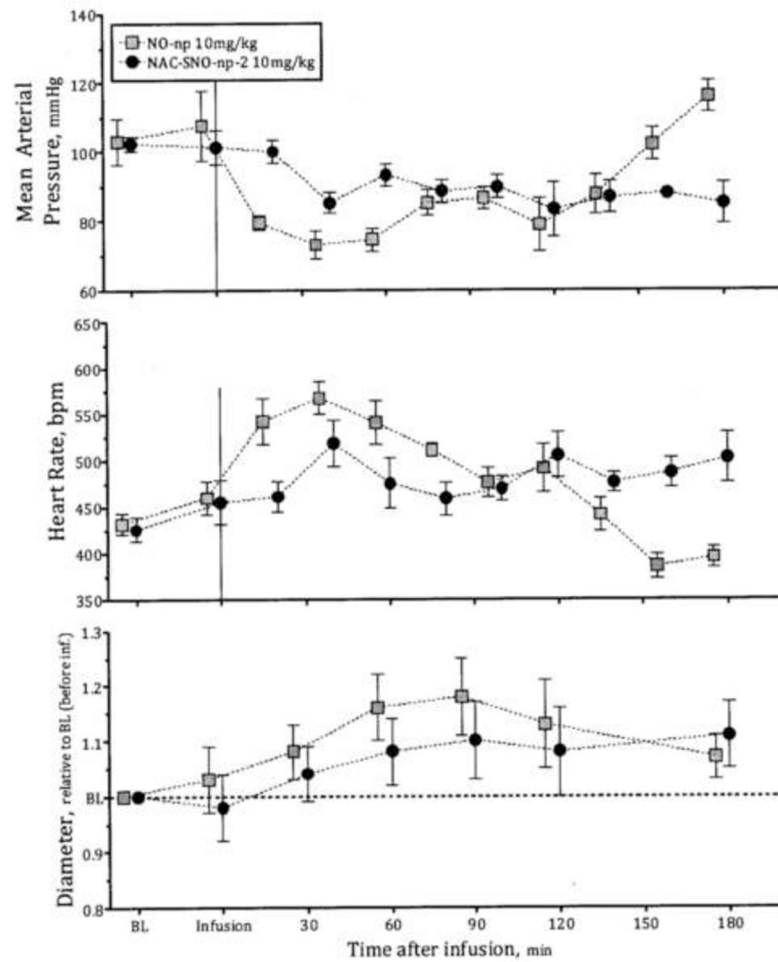


Figure 4. Vasodilatory effect of NO-np and NAC-SNO-np-2

Infusion of 10 mg/kg of NO-np and NAC-SNO-np-2 in hamsters reduced the mean arterial pressure and heart rate and increased vessel diameter. These changes induced by NAC-SNO-np-2 were lower but longer than NO-np. The effect of NO-np started diminishing after 2 h of infusion. NAC-SNO-np-2 maintained the effect until the termination of the experiment (3 h).

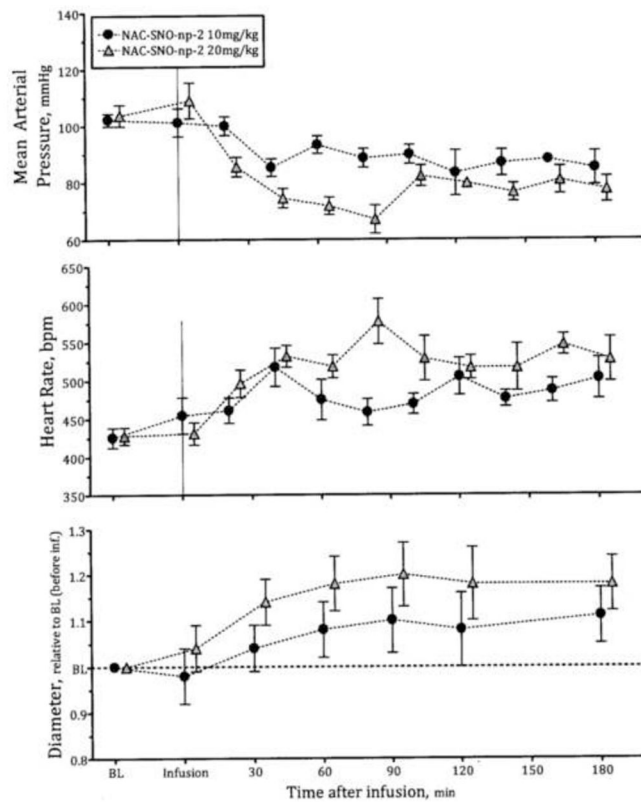


Figure 5. Dose dependent vasodilatory effect of NAC-SNO-np-2

Infusion of 10 and 20 mg/kg of NAC-SNO-np-2 in hamsters reduced the mean arterial pressure and heart rate and increased vessel diameter in a dose dependent fashion. Dose effects were more pronounced in microvessel diameter compared to systemic hemodynamics, suggesting specific vascular action on peripheral circulation.

Table 1

Nanoparticle formulations

Sample	[Nitrite] (M)	[D-glucose] (M)	[N-Ac-Cys] (M)	[Hydrolyzed MPTS] (M)	[Hydrolyzed TMOS] (M)	[Nitrite]:[Thiol]	Theoretical nitrite or SNO per mg of dry np (micromoles)
NO-np	0.225	0.055	N/A	N/A	0.68	N/A	0.75 (nitrite)
SNO-np	0.225	0.055	N/A	0.28	0.68	1:1.2	0.75 (SNO)
NAC-SNO-np-1	0.113	0.0275	0.28	N/A	0.68	1:2.5	0.375 (SNO)
NAC-SNO-np-2	0.225	0.055	0.28	N/A	0.68	1:1.25	0.75 (SNO)
NAC-SNO-np-3	0.450	0.110	0.28	N/A	0.68	1:0.625	1.50 (nitrite+SNO)

Table 2

GSNO production is dependent on Np and GSH concentration

Sample	Np (mg/ml)	Theoretical [nitrite] and/or [SNO] (mM)	[GSH] (mM)	[GSNO]* (mM)
NO-np	5	3.75	5	ND
“	10	7.50	10	ND
“	20	15.00	20	2.74
SNO-np	5	3.75	5	ND
“	10	7.50	10	ND
“	20	15.00	20	3.08
NAC-SNO-np-2	5	3.75	5	1.19
“	10	7.50	10	1.60
“	20	15.00	20	4.04

* GSNO formed after 1 hour incubation of Np with GSH in DTPA/PBS

ND = no GSNO peak was detected by RPHPLC

Table 3

Maximum GSNO formed from Np formulations

Sample	t MAX GSNO* (min)	[GSNO] (mM)	Percentage of nitrite/SNO converted to GSNO	[GSNO] after 24 h (mM)	Percentage of GSNO remained after 24 h
NO-np	60	2.74 (15) [#]	18	1.38	50
SNO-np	60	3.08 (15)	20	0.76	25
NAC-SNO-np-1	120	2.01 (7.5)	27	1.00	50
NAC-SNO-np-2	120	4.19 (15)	28	2.66	63
NAC-SNO-np-3	120	7.72 (30)	26	0.75	8

* Time at which maximum GSNO formed from np (20 mg/ml) and GSH (20 mM).

[#] The values in parentheses represent the initial concentration of nitrite and/or SNO of Nps
GSNO concentrations are the average of duplicate experiments.

Table 4

Blood chemistry

	Time after infusion, min	NO-np		NAC-SNO-np-2			
		10 mg/kg _{BW}		10 mg/kg _{BW}		20 mg/kg _{BW}	
		Baseline	60	60	180	60	180
MetHb, %	-0-	-0-	5 ± 2	-0-	3 ± 2	-0-	7 ± 3
NO ₃ ⁻ , μM	1.3 ± 0.3	2.8 ± 0.9 [†]	3.2 ± 0.8 [†]	1.6 ± 0.4 [‡]	1.7 ± 0.4 [†]	1.8 ± 0.5 [†]	2.0 ± 0.8 [†]
P _a O ₂ , mmHg	57.6 ± 7.6	76.2 ± 7.2 [†]	73.1 ± 6.7 [†]	59.3 ± 7.7 [‡]	58.4 ± 6.2 [‡]	62.4 ± 7.1 [†]	64.1 ± 7.2 [†]
P _a CO ₂ , mmHg	51.5 ± 5.6	47.8 ± 6.8 [†]	47.7 ± 5.8 [†]	49.2 ± 6.7 [‡]	49.8 ± 7.1 [‡]	47.5 ± 6.3	46.5 ± 4.7

Values are means ± SD. Baseline included all the animals. MetHb, fraction of Total Hb converted to Methemoglobin; NO₃⁻, Nitrate; P_aO₂, arterial partial O₂ pressure; P_aCO₂, arterial partial pressure of CO₂.

[†] P<0.05 compared to Baseline;

[‡] P<0.05 compared to NO-np at same concentration.